The Yang–Lee edge singularity in spin models on connected and non-connected rings

2008 J. Phys. A: Math. Theor. 41 505002

(http://iopscience.iop.org/1751-8121/41/50/505002)

IOP PUBLISHING JOURNAL OF PHYSICS A: MATHEMATICAL AND THEORETICAL

J. Phys. A: Math. Theor. **41** (2008) 505002 (15pp) doi:10.1088/1751-8113/41/50/505002

The Yang–Lee edge singularity in spin models on connected and non-connected rings

D Dalmazi and F L Sá

UNESP—Campus de Guaratinguetá, DFQ Av. Dr Ariberto P da Cunha, 333 CEP 12516-410, Guaratinguetá, SP, Brazil

E-mail: dalmazi@feg.unesp.br and ferlopessa@yahoo.com.br

Received 14 September 2008, in final form 8 October 2008
Published 3 November 2008
Online at stacks.iop.org/JPhysA/41/505002

Abstract

Renormalization group arguments based on a $\imath\varphi^3$ field theory lead us to expect a certain universal behavior for the density of partition function zeros in spin models with short-range interaction. Such universality has been tested analytically and numerically in different $d = 1$ and higher dimensional spin models. In $d = 1$, one finds usually the critical exponent $\sigma = -1/2$. Recently, we have shown in the $d = 1$ Blume–Emery–Griffiths (BEG) model on a periodic static lattice (one ring) that a new critical behavior with $\sigma = -2/3$ can arise if we have a triple degeneracy of the transfer matrix eigenvalues. Here we define the $d = 1$ BEG model on a dynamic lattice consisting of connected and non-connected rings (non-periodic lattice) and check numerically that also in this case we have mostly $\sigma = -1/2$ while the new value $\sigma = -2/3$ can arise under the same conditions of the static lattice (triple degeneracy) which is a strong check of universality of the new value of σ. We also show that although such conditions are necessary, they are not sufficient to guarantee the new critical behavior.

PACS numbers: 05.70.Jk, 05.50.+q, 05.70.Fh

(Some figures in this article are in colour only in the electronic version)

1. Introduction

The non-existence of real phase transitions in one-dimensional classical spin models with short-range interactions is a well-known fact in statistical mechanics. The free energy is analytic in the entire (real) parameters space of the model. However, if we let, for instance, the magnetic field H become a complex number, the analytic properties of the free energy change completely, since now we have complex, Yang–Lee [1] zeros for the partition function and consequently branch points for the free energy. In the thermodynamic limit, it is usually

possible to define a linear density of Yang–Lee zeros $\rho(H)$. Remarkably, the zeros accumulate at some special points, $H = H_E$, named Yang–Lee edge singularities [2], where the density diverges with an exponent σ, i.e., $\rho(H) \sim |H - H_E|^\sigma$ with $\sigma < 0$. As shown in [2] such behavior is presumably universal in each space dimension d above the critical temperature ($d \geqslant 2$) and for any $T > 0$ for $d = 1$. The critical properties of this special second-order phase transition are described by a $\imath\varphi^3$ field theory which leads to mean field results ($\sigma = +1/2$) for $d \geqslant 6$. In any dimension we can estimate σ perturbatively by an ϵ-expansion, with $\epsilon = 6 - d$, see [2, 3].

Since the Yang–Lee edge singularity is present in different space dimensions, the simplest case of one-dimensional models is a suitable laboratory for obtaining exact results and looking for new critical behaviors which would presumably appear also in higher dimensional models. In fact, one obtains $\sigma = -1/2$ exactly for the one-dimensional spin 1/2 Ising model with periodic boundary conditions (one ring) whose zeros are exactly known [1] for any finite number of spins. For the Q-state Potts model it is also possible to derive $\sigma = -1/2$ for any $Q \neq 1$ and positive [4]. The same value appears for the n-vector chain and Ising strips [5], with the help of numerical computations. In [5, 6], an attempt has been made, see also [7], to furnish a model independent demonstration that $\sigma = -1/2$ for one-dimensional spin models. The proof assumes that the magnetic field is pure imaginary, and the transfer matrix eigenvalues are real in the gap of zeros. Recently, another proof [8], which does not assume such hypotheses, has appeared; it also leads to $\sigma = -1/2$. In the present work, in particular, we have checked numerically that $\sigma = -1/2$ in most of the cases even if the magnetic field is not pure imaginary (no circle theorem).

Furthermore, inspired by [8] we have just shown in [9], for the one-dimensional Blume–Emery–Griffiths (BEG) and Blume–Capel (BC) models with periodic boundary conditions, that a new critical behavior with $\sigma = -2/3$ can appear if we fine tune the couplings of the model in such a way that has a triple degeneracy of the transfer matrix eigenvalues. In all of the above calculations of σ for one-dimensional spin models one assumes periodic boundary conditions. Here we analyze the effect of a particular dynamic (non-periodic) lattice on the critical exponent σ. The lattice consists of connected and non-connected rings, see [10], and corresponds to a one-dimensional version of statistical models on Feynman diagrams studied in [11, 12]. So, besides summing over spin degrees of freedom we also sum over all possible connected and non-connected rings with a given number of spins. The calculations, mostly numerical, of [10] for the Blume–Capel model indicate that the Yang–Lee zeros on the dynamic lattice tend to overlap with the static results (one ring) in the thermodynamic limit. The Yang–Lee zeros of the BEG model follow a similar pattern and, although the sum over polynomials (sum over rings) changes their zeros in a nontrivial way, we still have the usual critical behavior ($\sigma = -1/2$) and the new critical one ($\sigma = -2/3$) on the dynamic lattice as in the static case. This is a strong indication of the universality of the new critical behavior.

Last, it is important to mention that we study here a particular region in the parameters space of the BEG model (see subsection 3.2) where, differently from [9], the new edge singularity ($\sigma = -2/3$) is now the closest one to the positive real axis which is another hint that a new critical behavior at the edge singularity might appear also in higher dimensional spin models where a real phase transition takes places.

In the following section, we find an integral representation for the BEG model on connected and non-connected rings, see (6) and (7). We also show how to generalize the partition function of any one-dimensional spin model defined on a ring to connected and non-connected rings. Expressions (13) and (14) are the starting points for the numerical calculations of section 3, where we deduce the finite-size relations (24) and (25) necessary to obtain the exponents y_h, σ and the ratio $(y_h - d)/d$. In subsections (3.1) and (3.2) we

analyze two examples where $y_h \approx 2$ and $y_h \approx 3$ respectively. In section 4 we summarize our conclusions.

2. Spin models on non-connected rings

Originally, the BEG model has been introduced in [13] in order to describe phase separation driven by superfluidity in a mixture of He_3 and He_4 where each spin state $S_i = 0$ is associated with a He_3 atom while each atom of He_4 is equally described by $S = 1$ or $S = -1$. Differently from the original proposal we interpret here the BEG model as a generalization of the Blume–Capel [14] magnetic spin model where besides the dipole and quadrupole couplings, J and Δ respectively, one introduces another coupling constant K associated with a quartic spin interaction. Explicitly, we have

$$Z_N = \sum_{\{S_i\}} \exp\beta \left\{ J \sum_{\langle ij\rangle} S_i S_j + K \sum_{\langle ij\rangle} S_i^2 S_j^2 + \sum_{i=1}^{N} \left[H S_i + \Delta\left(1 - S_i^2\right)\right] \right\}. \quad (1)$$

Originally [13] the coupling H (magnetic field) is conjugated to the order parameter of superfluidity which corresponds to the magnetization in the magnetic spin model. The sums $\sum_{\langle ij\rangle}$ extend over nearest neighbor sites. On each of the N sites we can have $S_i = 0, \pm 1$. Henceforth, we assume ferromagnetic dipole coupling $J > 0$ while the signs of K and Δ are not fixed *a priori*. The couplings J, K, Δ and the temperature are all real but we allow the magnetic field H to be a complex number in general. We will be using the following notation :

$$c = \mathrm{e}^{-\beta J}, \quad b = \mathrm{e}^{\beta K}, \quad u = \mathrm{e}^{\beta H}, \quad x = \mathrm{e}^{\beta \Delta}, \quad \tilde{x} = xc = \mathrm{e}^{\beta(\Delta - J)}. \quad (2)$$

We measure the temperature in units of the ferromagnetic coupling J, i.e., the range $0 \leqslant T < \infty$ corresponds respectively to the compact interval $0 \leqslant c \leqslant 1$. We have chosen the BEG model since it is $\mathbb{Z}_2$ symmetric and includes interesting sub-models. For $\Delta = 0 = K\,(x = 1 = b)$ we recover the $S = 1$ Ising model while the $S = 1/2$ Ising model is obtained by freezing the $S_i = 0$ mode with $\Delta \to -\infty$ $(x \to 0)$. The BEG model contains also the $Q = 3$ states Potts model for $b = 1/c^3, \tilde{x} = u/c^3$ [15] and the Blume–Capel model for $b = 1$.

In order to define the partition function of the BEG model on non-connected rings we follow the same ideas used in the case of the BC model in [10]. We define the partition function by an expansion on Feynman diagrams. Namely, we first introduce three zero-dimensional fields ϕ_+, ϕ_-, ϕ_0 to describe the three spin states $S_i = +1, -1, 0$ respectively. We associate with each site with spin $S_i = +1, -1, 0$ a corresponding interaction vertex with two lines $\mathrm{e}^{\beta H}\phi_+^2$, $\mathrm{e}^{-\beta H}\phi_-^2$ and $\mathrm{e}^{\beta\Delta}\phi_0^2$ respectively, in accordance with the two terms inside the brackets in (1). Introducing a coupling constant g to bookkeep the number of sites (vertices) of the non-connected rings we can define the generating function of connected and non-connected rings

$$G = \sum_{N=0}^{\infty} g^N Z_N^{nc}, \quad (3)$$

via a Feynman integral which becomes in this case a triple integral on $\mathbb{R}_3$:

$$G = \frac{\int \mathrm{d}\phi_+\, \mathrm{d}\phi_-\, \mathrm{d}\phi_0\, \mathrm{e}^{-\frac{1}{2}[\phi_a M_{ab}\phi_b - g(\mathrm{e}^{\beta H}\phi_+^2 + \mathrm{e}^{-\beta H}\phi_-^2 + \mathrm{e}^{\beta\Delta}\phi_0^2)]}}{\int \mathrm{d}\phi_+\, \mathrm{d}\phi_-\, \mathrm{d}\phi_0\, \mathrm{e}^{-\frac{1}{2}[\phi_a M_{ab}\phi_b]}}. \quad (4)$$

In (3) we have $Z^{nc}_{N=0} = 1$. The repeated indices $a, b = +, -, 0$ are summed over. The 3×3 symmetric matrix M_{ab} is determined by associating each Boltzmann weight of a link which connects the spins S_a and S_b to a propagator $\langle \phi_a \phi_b \rangle$, namely,

$$M^{-1}_{ab} = \langle \phi_a \phi_b \rangle = \kappa \, \mathrm{e}^{\beta J S_a S_b + \beta K S_a^2 S_b^2}. \tag{5}$$

The overall constant κ is not fixed *a priori*. By using $\kappa = (b/c^2)(1-c^2)[b(1+c^2) - 2c]$ we find the following integral representation for the generating function G:

$$G = \frac{\int \mathrm{d}\phi_+ \, \mathrm{d}\phi_- \, \mathrm{d}\phi_0 \, \mathrm{e}^{-S_g}}{\int \mathrm{d}\phi_+ \, \mathrm{d}\phi_- \, \mathrm{d}\phi_0 \, \mathrm{e}^{-S_{g=0}}} \tag{6}$$

with the 'action' defined by

$$S_g = \tfrac{1}{2} \left\{ A \left(\phi_+^2 + \phi_-^2 \right) + 2B\phi_+\phi_- + D \left[E\phi_0^2 + 2\phi_0(\phi_+ + \phi_-) \right] \right\} + \frac{g}{2} \left(\mathrm{e}^{\beta H} \phi_+^2 + \mathrm{e}^{-\beta H} \phi_-^2 + \mathrm{e}^{\beta \Delta} \phi_0^2 \right), \tag{7}$$

where $A = -1 + \frac{b}{c}$, $B = 1 - cb$, $D = b\left(c - \frac{1}{c}\right)$ and $E = -b\left(c + \frac{1}{c}\right)$. Expressions (3), (6) and (7) define an integral representation for the partition functions Z^{nc}_N of the BEG model on connected and non-connected rings. At this point one could simply calculate the Gaussian integrals in (6) and find an explicit representation for the partition functions Z^{nc}_N of the BEG model. We follow instead a different route which can be easily generalized to other spin models.

It is known in diagrammatic expansions, see e.g. [16], that if we take the logarithm of the generating function G we end up with only connected diagrams. In our case, we have only one connected diagram which is the usual ring, i.e., a 1D lattice with periodic boundary conditions $S_i = S_{i+N}$. Including the proportionality constant κ and the symmetry factor $2N$ of a connected ring (one ring) with N vertices (sites) we have

$$\ln G = \sum_{N=1}^{\infty} \frac{(\kappa g)^N}{2N} Z_N. \tag{8}$$

From (3) and (8) we find a formula for Z^{nc}_N in terms of the usual (one ring) partition functions for the 1D spin model, namely[1],

$$Z^{nc}_N = [\mathrm{e}^{\ln G}]_{g^N} = \left[\exp \sum_{m=1}^{\infty} \frac{(\kappa g)^m}{2m} Z_m \right]_{g^N} = \kappa^N \left[\frac{Z_1^N}{2^N N!} + \cdots + \frac{Z_1 Z_{N-1}}{4(N-1)} + \frac{Z_N}{2N} \right]. \tag{9}$$

Compare formula (9) for $N = 4$ with figure 1. From (1) we see that Z_N is proportional to a polynomial of degree $2N$ in the variable $u = \exp(\beta H)$. Since the addition of polynomials changes their zeros in a nontrivial way, we see from (9) that the Yang–Lee zeros of the model on the dynamic lattice are in principle quite different from their static counterpart. However, the numerical results show that they remain quite close to each other, see figure 3. Note that although the last term on the right-hand side of (9) contains the largest overall numerical factor for large N, the numerical factor of the term before the last is of the same order of the last one for $N \to \infty$; thus, it is not clear why the position of the zeros is so similar in both cases of Z_N and Z^{nc}_N.

The relationship (9) can be considered the general definition of Z^{nc}_N for any 1D spin model with nearest neighbor interactions whose original partition functions (periodic boundary

[1] Throughout this work the notation $[f(g)]_{g^N}$ stands for the coefficient of the term of power g^N in the Taylor expansion of $f(g)$ about $g = 0$.

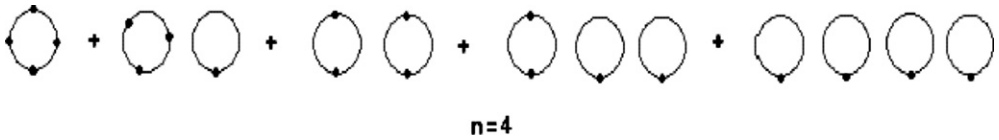

Figure 1. Feynman diagrams for Z_4^{nc}.

conditions) are defined by Z_N. Since each of the partition functions Z_N can be written in terms of transfer matrix eigenvalues $Z_N = \tilde{\lambda}_1^N + \tilde{\lambda}_2^N + \cdots + \tilde{\lambda}_Q^N$, where Q is the size of the transfer matrix, we can find, as we show next, an expression for Z_N^{nc} also in terms of the eigenvalues $\tilde{\lambda}_i$ which are the roots of the secular equation

$$P_Q(\tilde{\lambda}) \equiv \tilde{\lambda}^Q + a_{Q-1}\tilde{\lambda}^{Q-1} + \cdots + a_1\tilde{\lambda} + a_0 = 0. \tag{10}$$

The coefficients $a_i, i = 1, \ldots, Q-1$ depend upon the parameters of the specific spin model.

From (8) we have, below $\tilde{g} = \kappa g$,

$$\begin{aligned} \ln G &= \sum_{N\geqslant 1} \frac{(\kappa g)^N}{2N}\left(\tilde{\lambda}_1^N + \tilde{\lambda}_2^N + \cdots + \tilde{\lambda}_Q^N\right) \\ &= -\frac{1}{2}\ln\prod_{i=1}^{Q}(1-\tilde{\lambda}_i\tilde{g}) = -\frac{1}{2}\ln\left[\tilde{g}^Q\prod_{i=1}^{Q}\left(\frac{1}{\tilde{g}}-\tilde{\lambda}_i\right)\right] \\ &\equiv -\frac{1}{2}\ln R_Q(\tilde{g}). \end{aligned} \tag{11}$$

Since $\tilde{\lambda}_i$ are the roots of (10), the polynomial $R_Q(\tilde{g})$ is proportional to (10), i.e.,

$$R_Q(\tilde{g}) = \tilde{g}^Q P_Q\left(\frac{1}{\tilde{g}}\right). \tag{12}$$

By comparing (8) with (11) we obtain the following general formula for the partition functions Z_N (one ring):

$$Z_N = -N\{\ln[R_Q(\tilde{g})]\}_{\tilde{g}^N}. \tag{13}$$

Analogously, from (3) and the exponential of (11) we deduce for Z_N^{nc} (connected and non-connected rings)

$$Z_N^{nc} = \{[R_Q(\tilde{g})]^{-1/2}\}_{\tilde{g}^N}. \tag{14}$$

We have suppressed an overall constant κ^N in (14). In conclusion, all we need to compute the finite-size partition functions Z_N and Z_N^{nc} is the secular equation (10) of the corresponding 1D spin model with periodic boundary conditions. Formulae (13) and (14) will be used throughout this work in order to find the Yang–Lee zeros of the $d = 1$ BEG model on the static (one ring) and dynamic (connected and non-connected rings) lattices but they could be used equally well for finding the Yang–Lee zeros of any other spin model whose secular equation is known.

We remark that, for computational purposes, formula (13) turns out to be much more efficient than the traditional transfer matrix solution $Z_N = \tilde{\lambda}_1^N + \tilde{\lambda}_2^N + \cdots + \tilde{\lambda}_Q^N$, specially for large N. It is also important to note that for higher spin models $S \geqslant 2$ ($Q \geqslant 5$) no analytic solution for the roots of a degree 5 or higher polynomial is known in general, so we have to fix numerical values for the coefficients a_i of the secular equation (10) in order to find the eigenvalues $\tilde{\lambda}_i, i = 1, \ldots, Q$. However, since some of the coefficients depend upon the magnetic field this implies the assignment of numerical values for the magnetic field itself.

Therefore, we will not be able to find the eigenvalues as functions of the magnetic field ($\tilde{\lambda}_i = \tilde{\lambda}_i(h)$), and consequently we cannot derive an explicit formula for the partition function as a function of the magnetic field via $Z_N = \tilde{\lambda}_1^N(h) + \tilde{\lambda}_2^N(h) + \cdots + \tilde{\lambda}_Q^N(h)$. Instead, one could use $Z_N = \mathrm{tr}(T^N)$ since we know the $Q \times Q$ transfer matrix T explicitly for each spin model. Some tests with the software Mathematica show that (13) is computationally more efficient.

3. Finite-size scaling relations and numerical results

We have found convenient to redefine the transfer matrix eigenvalues $\tilde{\lambda}_i = \lambda_i/c$ such that $Z_N = c^{-N}\left[\lambda_1^N + \lambda_2^N + \lambda_3^N\right]$. The λ_i are the roots of the redefined secular equation

$$\lambda^3 - a_2\lambda^2 + a_1\lambda - a_0 = 0, \tag{15}$$

with, see [7, 9], the coefficients

$$\begin{aligned} a_0 &= b\tilde{x}(1-c^2)[b(1+c^2) - 2c], \\ a_1 &= b^2(1-c^4) + A\tilde{x}(b-c), \\ a_2 &= \tilde{x} + Ab, \end{aligned} \tag{16}$$

and

$$A = u + 1/u = 2\cosh\beta H. \tag{17}$$

Note that the $\mathbb{Z}_2$ symmetry $H \to -H$ ($u \to 1/u$) is explicit. Back to formulae (12), (13) and (14) we have for the BEG model

$$R_3(\tilde{g}) = 1 - a_2\tilde{g} + a_1\tilde{g}^2 - a_0\tilde{g}^3, \tag{18}$$

$$Z_N = -Nc^{-N}\{\ln[R_3((\tilde{g})]\}_{\tilde{g}^N}, \tag{19}$$

$$Z_N^{nc} = c^{-N}\{[R_3((\tilde{g})]^{-1/2}\}_{\tilde{g}^N}. \tag{20}$$

Formulae (18), (19) and (20) can be easily implemented in the computer. Fixing numerical values for the couplings b, c, x we can find the Yang–Lee zeros numerically. In order to obtain the magnetic scaling exponent y_h from the Yang–Lee zeros we use two finite-size scaling relations which read [17, 18], dropping corrections to scaling,

$$u_1(N) - u_1(\infty) = \frac{C_1}{L^{y_h}} = \frac{C_1}{N^{y_h/d}}, \tag{21}$$

$$\rho(N) = C_2 L^{y_h - d} = C_2 N^{(y_h-d)/d}, \tag{22}$$

where C_1 and C_2 are in general complex constants, independent of the number of spins $N = L^d$. The quantity $u_1(N)$ is the closest Yang–Lee zero to the edge singularity $u_E = u_1(\infty)$ for N spins. The linear density $\rho(N)$ is the normalized density of Yang–Lee zeros calculated at $u_1(N)$. In practice, we use the first two closest Yang–Lee zeros $u_1(N)$ and $u_2(N)$ to compute $\rho(N)$:

$$\rho(N) = \frac{1}{N|u_1(N) - u_2(N)|}. \tag{23}$$

By comparing two lattices of different sizes N_a and N_{a+1} we can deduce from (21) and (22) respectively,

$$\frac{y_h}{d} = -\left[\ln\frac{N_{a+1}}{N_a}\right]^{-1} \ln\left[\frac{\Delta u_E(N_{a+1})}{\Delta u_E(N_a)}\right], \tag{24}$$

$$\frac{y_h - d}{d} = \left[\ln \frac{N_{a+1}}{N_a}\right]^{-1} \ln\left[\frac{\rho(N_{a+1})}{\rho(N_a)}\right], \tag{25}$$

where we may use either $\Delta u_E(N) = \mathrm{Im}(u_1(N) - u_E)$ or $\Delta u_E(N) = \mathrm{Re}(u_1(N) - u_E)$.

In order to use (24) we must know the position of the Yang–Lee edge singularity $u_E = u_1(\infty)$. Since the coincidence of the two largest eigenvalues of the transfer matrix leads to phase transition [19, 20] for a static lattice (one ring), we can find u_E in this case from the double degeneracy condition of the cubic equation (15), which is , see also [7],

$$27a_0^2 + 4a_1^3 + 4a_2^3 a_0 - a_1^2 a_2^2 - 18a_0 a_1 a_2 = 0. \tag{26}$$

Expression (26) leads to four solutions for $A_E = u_E + 1/u_E$ and therefore eight solutions for u_E. After checking, for each solution, that the degenerate eigenvalues are indeed the largest ones and not the smallest ones, and overlapping them with the real curve of zeros we did not have any difficult in identifying u_E. Regarding the second scaling relation (25), once again for the static case the situation is simpler. We can simply fix the space dimension $d = 1$ and consider (25) an independent source of a numerical estimate of y_h.

The case of the dynamic lattice is more complicated. The integral representation (4) allows us to use a saddle point argument, similar to that used in the Blume–Capel case in [10], which lead us to believe that the position of the Yang–Lee edge singularity for the dynamic case coincides with u_E found from the double degeneracy condition (26). We have no rigorous proof of this fact. Based on this hypothesis we have calculated y_h/d for the dynamic case from (24). Furthermore, since the lattice itself is a degree of freedom it is not clear now whether $d = 1$ still holds. In practice, one can use the second scaling relation (25) to compute $(y_h - d)/d$ and from both results one finds y_h and d separately.

Next we analyze two subcases of the BEG model both on the static and dynamic $d = 1$ lattice and for different temperatures. The first case leads to the traditional result $\sigma = -1/2$ while in the second one the conditions for a triple degeneracy of the transfer matrix eigenvalues are satisfied, and we have a new critical behavior $\sigma = -2/3$ for all temperatures except $c = \sqrt{2}/2 \approx 0.707$ where we are back to $\sigma = -1/2$.

3.1. *Case I* ($\sigma = -1/2$): $(b, \tilde{x}) = (2, 2.5)$

Earlier proofs that $\sigma = -1/2$ in 1D spin models, see [5–7], assume that the magnetic field is pure imaginary $\beta H = \imath\alpha$, i.e., the Yang–Lee zeros lie on the unit circle on the complex fugacity plane ($|u| = |e^{\imath\alpha}| = 1$). Technically, this assumption implies that the $\mathbb{Z}_2$ invariant combination $A = u + 1/u = 2\cos\alpha$ is real, which guarantees that the coefficients of the cubic equation (15) are also real and the complex eigenvalues must appear in complex conjugated pairs, so they must share the same absolute value which facilitates the proofs. One exception is the one-dimensional Q-state Potts model whose zeros are not on the unit circle for $Q \neq 2$ but we still have, see [4], $\sigma = -1/2$ for any positive $Q \neq 1$. In the recent proof [8] of $\sigma = -1/2$ for the 1D Blume–Capel model there is no need for a pure imaginary magnetic field although there are other implicit assumptions. Since the Yang–Lee zeros for the BEG model, see [10, 15], are not always on the unit circle it is of interest to check numerically if we still have $\sigma = -1/2$ as predicted in [8], for a case where the zeros do not lie on the unit circle. As such example we can take $b = 2$ and $\tilde{x} = 5/2$. For this choice it is also possible to prove that no triple degeneracy of the transfer matrix eigenvalues is possible for real temperatures; thus, there will be no crossover to $\sigma = -2/3$. Of course, those arguments are only rigorously correct for the static case.

For $b = 2$ and $\tilde{x} = 5/2$ half of the Yang–Lee zeros are inside the unit circle and the other half outside, see figure 2. Only half of the eight solutions of the double degeneracy

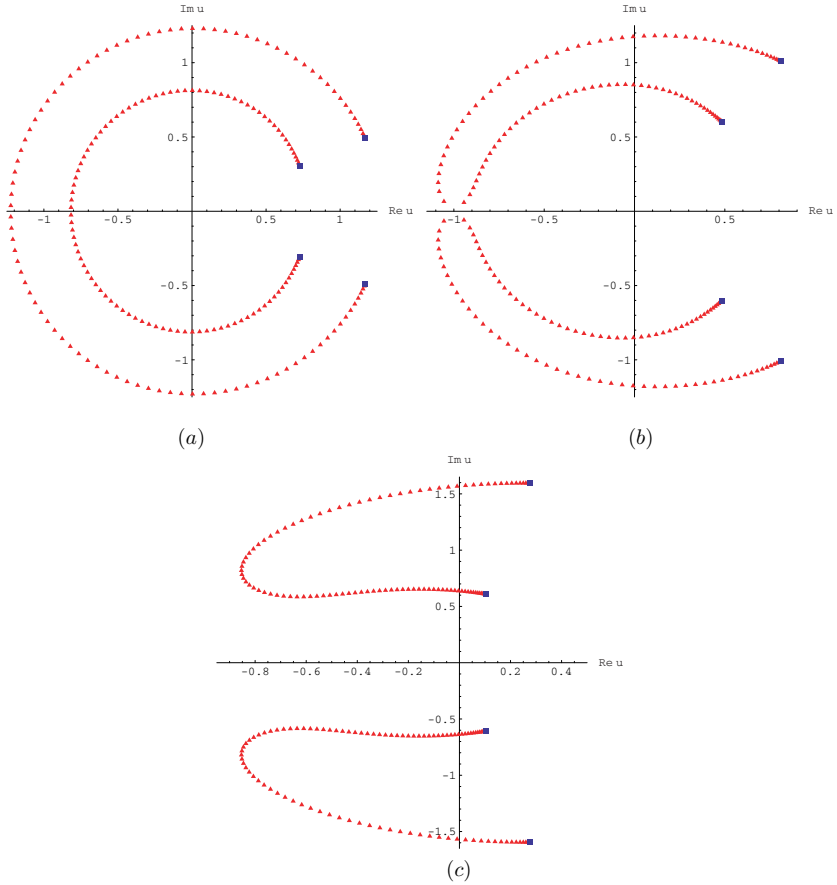

Figure 2. Yang–Lee zeros for the BEG model with $b = 2$ and $\tilde{x} = 2.5$ on the complex u-plane ($u = \mathrm{e}^{-\beta H}$), at $c = 0.1$ (figure 1), $c = 0.5$ (figure 2) and $c = 0.9$ (figure 3). In the figures we have $N = 100$ zeros. The edges are represented by squares.

condition (26) correspond to true Yang–Lee edge singularities, as shown in figure 2. Under $\mathbb{Z}_2$ symmetry we have $u = \mathrm{e}^{\beta(H_R + \imath H_I)} \to 1/u = \mathrm{e}^{\beta(-H_R - \imath H_I)}$, therefore, the outer edge on the upper half-plane is $\mathbb{Z}_2$ conjugated to the inner edge on the lower half-plane and vice-versa. We also observe in figure 2 that by increasing the temperature the edges move in the anticlockwise direction. Defining $u = \rho\,\mathrm{e}^{\imath\alpha}$, the two approximate circles with $\rho > 1$ (outer) and $\rho < 1$ (inner) split into two new curves on the upper and lower half-planes, respectively at some temperature close to $c = 0.5$. The results on the dynamic lattice look quite similar to the static case. In figure 3, we overlap the zeros for both cases at $c = 0.6$.

In table 1, we display the finite-size results obtained from formulae (24) and (25) for the inner edge in both cases of static and dynamic lattices. We have determined the positions of the Yang–Lee edge singularity $u_E = u_1(\infty)$ for the static case from the double degeneracy condition (26) and assumed the same value for non-connected rings[2]. For the outer edge

[2] Alternatively, we have made a three parameters fit of (21) to obtain $C_1, u_1(\infty), y_h/d$. However, the quality of the fit, measured by χ^2, is in all cases worse (larger χ^2) than a two parameters fit of (21) for C_1 and y_h/d with a given value of $u_1(\infty)$ determined from (26).

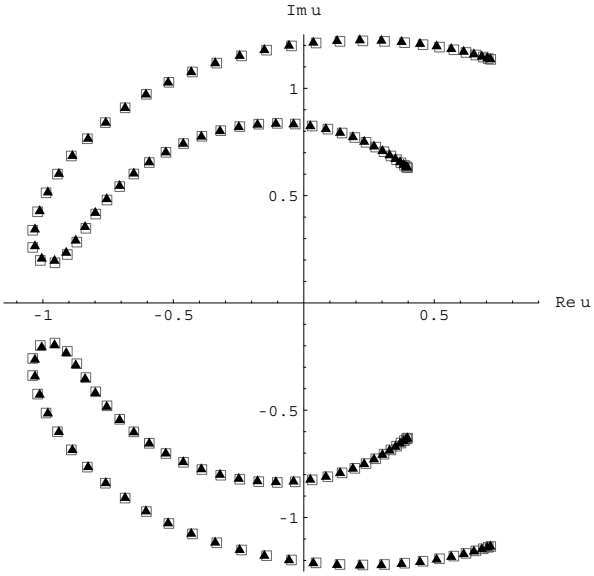

Figure 3. Yang–Lee zeros for the BEG model with $b = 2$ and $\tilde{x} = 2.5$ on the complex u-plane ($u = \mathrm{e}^{-\beta H}$), at $c = 0.6$, with $N = 60$ zeros. The zeros on the static (dynamic) lattice are represented by empty squares (triangles).

Table 1. Finite-size results for the BEG model with $b = 2$ and $\tilde{x} = 2.5$ at the temperature $c = 0.6$ and $110 \leqslant N \leqslant 190$ spins (inner edge).

N_a	y_h (static)	y_h/d (dynamic)	$y_h - 1$ (static)	$(y_h - d)/d$ (dynamic)
150	1.991 539 508 388	1.992 328 729 234	0.991 539 508 388	0.992 328 729 234
160	1.999 444 980 343	1.992 843 330 971	0.999 444 980 343	0.992 843 330 971
170	1.999 510 053 393	1.993 293 645 217	0.999 510 053 393	0.993 293 645 217
180	1.999 564 326 434	1.993 690 952 252	0.999 564 326 434	0.993 690 952 252
190	1.999 610 062 131	1.994 044 049 618	0.999 610 062 131	0.994 044 049 618
200	1.999 648 960 537	1.994 359 897 273	0.999 648 960 537	0.994 359 897 273
210	1.999 682 318 897	1.994 644 072 074	0.999 682 318 897	0.994 644 072 074
220	1.999 711 140 922	1.994 901 094 084	0.999 711 140 922	0.994 901 094 084
230	1.999 736 212 993	1.995 134 664 894	0.999 736 212 993	0.995 134 664 894

singularity ($\rho > 1$) we have found similar results. We note that, although we have taken the real part of the finite-size relation (21) if we replace it by the imaginary part instead, not displayed, the differences are negligible.

In order to extrapolate our finite-size results to $N \to \infty$ we use the BST algorithm [21, 22]. We assume that there is an expansion:

$$y_h(N) = y_h(\infty) + \frac{A_1}{N^w} + \frac{A_2}{N^{2w}} + \cdots . \tag{27}$$

The BST extrapolation consists of approximating the function $y_h(N)$ by a sequence of ratios of polynomials with a faster convergence than the original sequence $y_h(N_a)$. The parameter w is not fixed *a priori*. One can define, see [22, 23], the best value for w by minimizing the uncertainty of the method which is twice the difference between the two approximants

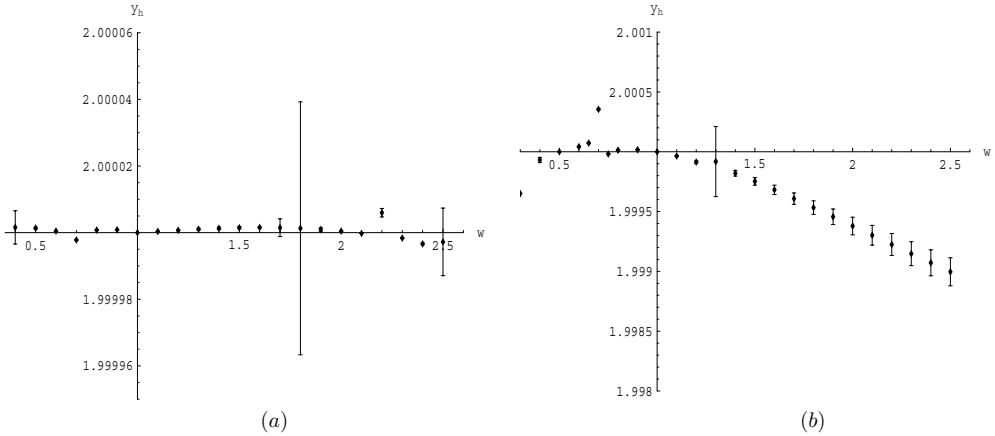

Figure 4. BST extrapolation of y_h/d and its uncertainties for the BEG model with $b = 2$ and $\tilde{x} = 2.5$ as a function of the BST parameter ω for the static (a) and dynamic (b) lattices at $c = 0.6$ (inner edge).

Table 2. BST extrapolations of y_h/d, with the BST parameter $\omega = 1$, for the BEG model with $b = 2$ and $\tilde{x} = 2.5$ at edges inside (inner) and outside (outer) the unit circle at different temperatures.

c	0.1	0.6	0.9
$y_h(\infty)$ (outer/static)	2.000 000 000 01(2)	1.999 999 999 9999(5)	1.999 999 999 9999(2)
$y_h(\infty)/d$ (outer/dynamic)	2.000 000 0008(4)	2.000 000 000 00(1)	2.000 000 000 0000(6)
$y_h(\infty)$ (inner/static)	1.999 999 9997(8)	2.000 000 000 00(4)	1.999 999 999 999(2)
$y_h(\infty)/d$ (inner/dynamic)	2.000 000 000(4)	1.999 999 999 99(2)	2.000 000 000 000(2)

Table 3. BST extrapolations of $(y_h - d)/d$, with the BST parameter $\omega = 1$, for the BEG model with $b = 2$ and $\tilde{x} = 2.5$ at edges inside (inner) and outside (outer) the unit circle at different temperatures.

c	0.1	0.6	0.9
$y_h - 1$ (outer/static)	1.000 000 000 01(2)	0.999 999 999 9999(5)	0.999 999 999 9999(2)
$(y_h^{(\rho)}(\infty) - d)/d$ (outer/dynamic)	1.000 000 0008(4)	1.000 000 000 00(1)	1.000 000 000 0000(6)
$y_h - 1$ (inner/static)	0.999 999 9997(8)	1.000 000 000 00(4)	0.999 999 999 999(2)
$(y_h^{(\rho)}(\infty) - d)/d$ (inner/dynamic)	1.000 000 000(4)	0.999 999 999 99(2)	1.000 000 000 000(2)

appearing in the last sequence before the final extrapolated result $y_h(\infty)$. In figures 4(a) and 4(b), we display both $y_h(\infty)$ and the uncertainty (error bars) as a function of the free parameter w. The value $w = 1$ seems to be the stablest one, so we use $w = 1$ henceforth. All results in tables 2 and 3 are consistent with $y_h = 2$ and $d = 1$ for the static and dynamic lattices. Therefore, we conclude that $\sigma = (d - y_h)/y_h = -1/2$ for both the static and the dynamic cases even though the magnetic field is not pure imaginary, which is in agreement with the demonstration of [8] which assumes a usual transfer matrix solution (one ring).

3.2. Case II ($\sigma = -2/3$): $\lambda_1 = \lambda_2 = \lambda_3$ and $\beta H = \pm\imath\pi/2$

We have shown in [9], for the static case, that we might have a new critical behavior at the Yang–Lee edge singularity in one-dimensional spin models if we fine tune the parameters of the model in such a way that a triple degeneracy of the solutions of the cubic equation (15) is achieved. This requires $3a_1 = a_2^2$ and $a_1 a_2 = 9a_0$, which can be written respectively as

$$\tilde{x}^2 + b^2A^2 + A\tilde{x}(3c - b) - 3b^2(1 - c^4) = 0, \tag{28}$$

$$(b - c)A\tilde{x}\,(\tilde{x} + bA) + b^3(1 - c^4)A = b(1 - c^2)[8b(1 + c^2) - 18c]\tilde{x}. \tag{29}$$

An interesting solution of (28) and (29) comes out when we fix the Yang–Lee edge singularity at $A = 0$ which corresponds to $\beta H = \pm\imath\pi/2$. In this case, (28) and (29) imply

$$b = \frac{9c}{4(1 + c^2)}, \tag{30}$$

$$\tilde{x} = b\sqrt{3(1 - c^4)} = \frac{9c}{4}\sqrt{\frac{3(1 - c^2)}{1 + c^2}}. \tag{31}$$

In [9], in order to have a new critical behavior with $\sigma = -2/3 (y_h = 3)$, besides the triple degeneracy conditions (28) and (29) we have also assumed $\tilde{x} \neq \bar{x}$ where $\bar{x} = (1-c^2)b^2/|b-c|$. Otherwise, $\lambda_1 = \tilde{x}(b - c)/b$ becomes a solution of (15) and consequently we may no longer have, see [9], $y_h = 3$. By matching $\bar{x}$ with $\tilde{x}$ given in (31) we find out the real temperature $c = \sqrt{2}/2 \approx 0.707$ which requires special care. In particular, it is possible to prove exactly that $y_h = 2$ when $c = \sqrt{2}/2$, and conditions (30) and (31) are satisfied as we show next. This special point in the parameters space of the BEG model is similar to the $Q = 3$ states Potts model, where one transfer matrix eigenvalue is independent of the magnetic field and the two remaining ones acquire a simple form. Plugging $c = \sqrt{2}/2$ and b , $\tilde{x}$ given by (30) and (31) in (15) we find the simple solutions

$$\lambda_1 = \frac{\tilde{x}(b - c)}{b} = \frac{3}{4\sqrt{2}}, \tag{32}$$

$$\lambda_2 = \frac{3}{4\sqrt{2}}[1 + A + \sqrt{A(A + 2)}], \tag{33}$$

$$\lambda_3 = \frac{3}{4\sqrt{2}}[1 + A - \sqrt{A(A + 2)}]. \tag{34}$$

Following [8, 9], imposing that $\lambda_1 = \mathrm{e}^{\imath\varphi}\lambda_2$ we derive $A = -1 + \cos\varphi$ and the three eigenvalues will have the same magnitude since $\lambda_3 = \lambda_1\,\mathrm{e}^{\imath\varphi}$. Consequently, $Z_N = c^{-N}\left[\lambda_1^N + \lambda_2^N + \lambda_3^N\right] = c^{-N}\lambda_1^N\,[1 + 2\cos N\varphi]$. Therefore, $Z_N = 0$ leads to $\varphi_k = 2\pi(3k + 1)/3N$ with $k = 0, 1, \ldots, N - 1$. So the $2N$ zeros of Z_N are determined exactly and uniquely from

$$A_k = -1 + \cos\varphi_k, \qquad \varphi_k = \frac{2\pi}{3N}(3k + 1), \qquad k = 0, 1, \ldots, N - 1. \tag{35}$$

Thus, we know the exact position of the partition function zeros for the static case and finite N at the temperature $c = \sqrt{2}/2$ with $b, \tilde{x}$ given by (30) and (31).

The Yang–Lee edge singularity occurs in this case at the triple degeneracy point $\lambda_1 = \lambda_2 = \lambda_3$, i.e., $\varphi = 0$ which implies $A = 0 (u_E = \pm\imath)$. Therefore, it is natural to suppose that the smallest phase $\varphi_0 = 2\pi/3N$ corresponds to the closest zero to the Yang–Lee edge singularity. This is in agreement with our numerical calculations. Consequently,

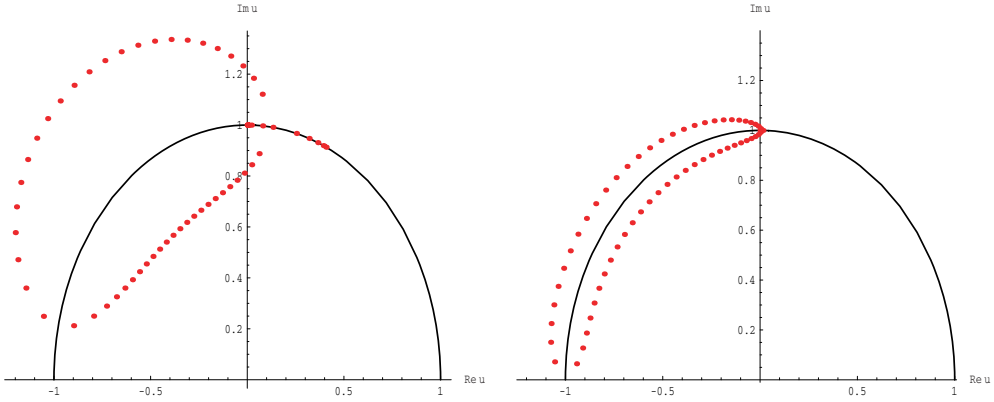

Figure 5. Yang–Lee zeros for the BEG model with $b = 9c/4(1 + c^2)$ and $\tilde{x} = b\sqrt{3(1 - c^4)}$ on the upper half complex u-plane ($u = \mathrm{e}^{-\beta H}$), at $c = 0.1$ (a) and $c = 0.65$ (b). In the figures, we have $N = 60$ zeros, and the solid curve stands for the unit circle.

inverting the relation $u + 1/u = A_0$ we have the following large N expansion for the closest zero to the Yang–Lee edge singularity and its complex conjugated:

$$u_1^{\pm}(N) = \frac{1}{2}\left[A_0 \pm \sqrt{A_0^2 - 4}\right]$$
$$\approx \pm\imath - \frac{1}{4}\left(\frac{2\pi}{3N}\right)^2 + \left(\frac{1}{48} \mp \frac{\imath}{32}\right)\left(\frac{2\pi}{3N}\right)^4 + \cdots. \tag{36}$$

A comparison with (21) leads exactly to $y_h = 2$ and consequently $\sigma = -1/2$ for the static case at the special temperature $c = \sqrt{2}/2$.

As explained in [9], although the cubic equation can be exactly solved for any temperature, the explicit solutions are so complicated in general that the above arguments cannot be repeated, so we have to stick to numerical calculations even in the static case for $c \neq \sqrt{2}/2$. Before we go on, it is important to mention that our numerical calculations of the Yang–Lee zeros for the static case, at the special case $c = \sqrt{2}/2$, are in agreement with the exact results (35) within the first 30 digits for $N \leqslant 150$ spins.

For b and $\tilde{x}$ given in (30) and (31) we have verified numerically that for $c < \sqrt{2}/2$ only a small fraction of the Yang–Lee zeros lies on the unit circle S_1 ($|u| = 1$), see figure 5(a), forming a short arc of zeros. The curve of zeros which are not on S_1, if analytically continued at the top crossing point with S_1, splits the short arc of zeros into two different sequences of zeros which tend to accumulate at two different Yang–Lee edge singularities. Namely, the left edge of the arc approaches $u_E = \imath (A = 0)$ in the anticlockwise direction, as we increase the number of spins, while the right edge approaches another singularity $\tilde{u}_E$ in the clockwise direction. As we increase the temperature $c \to (\sqrt{2}/2)^-$ we note that $\tilde{u}_E \to u_E$ and the fraction of zeros on the unit circle decreases. It turns out that the right edge singularity $\tilde{u}_E$ is of the usual type with $y_h \approx 2 (\sigma \approx -1/2)$, as we have checked numerically, while for $u_E = \imath$ we have found $y_h \approx 3 (\sigma \approx -2/3)$. There are no edge singularities outside the unit circle. However, the zeros out of S_1 all move to S_1 as $c \to (\sqrt{2}/2)^-$. We find out numerically that all zeros belong to S_1 for $c \geqslant \sqrt{2}/2$ which is in agreement with the analytic result (35) at the special point $c = \sqrt{2}/2$. At $c = \sqrt{2}/2$, for both static and dynamic cases, the Yang–Lee zeros seem to have a pairwise behavior, see figure 6. For $c > \sqrt{2}/2$, as we increase the temperature

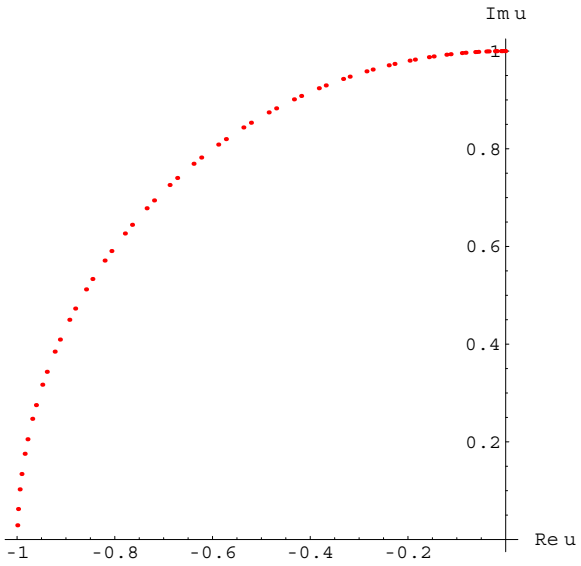

Figure 6. Yang–Lee zeros for the BEG model with $b = 9c/4(1 + c^2)$ and $\tilde{x} = b\sqrt{3(1 - c^4)}$ on the upper half complex u-plane ($u = e^{-\beta H}$), at $c = \sqrt{2}/2$. In the figure we have $N = 60$ zeros.

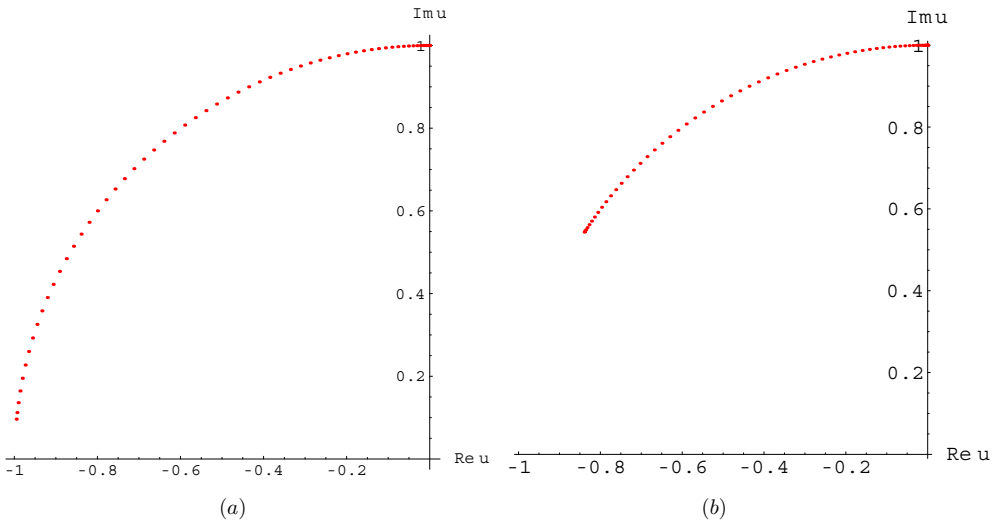

Figure 7. Yang–Lee zeros for the BEG model with $b = 9c/4(1 + c^2)$ and $\tilde{x} = b\sqrt{3(1 - c^4)}$ on the upper half complex u-plane ($u = e^{-\beta H}$), at $c = 0.75$ (a) and $c = 0.9$ (b). In both figures we have $N = 60$ zeros.

the size of the arc of zeros on S_1 decreases, see figure 7. In table 4, we display our final extrapolated results for the magnetic scaling exponent y_h. Our results for $c > \sqrt{2}/2$ show that the right edge $u_E = \iota$ possesses a new critical behavior with $y_h \approx 3$, see figures 8(a) and 8(b). For the left edge we have the usual result $y_h \approx 2$. So the new critical behavior, contrary to the cases treated in [9], now appears at the closest edge to the positive real axis. Note also that the dynamics of the lattice did not change the critical behaviors at the edges.

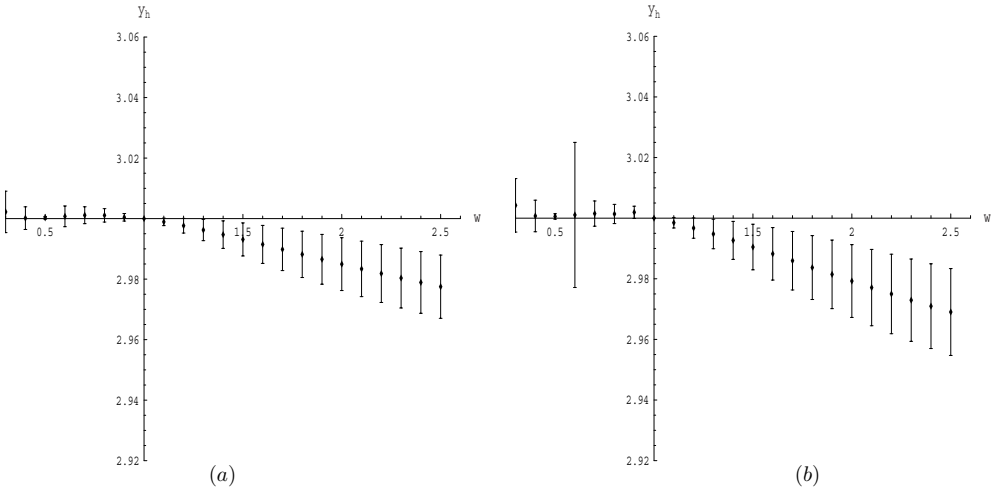

Figure 8. BST extrapolation of y_h/d and its uncertainties for the BEG model with $b = 9c/4(1+c^2)$ and $\tilde{x} = b\sqrt{3(1-c^4)}$ for zeros close to the edge $u_E = \mathrm{i}$, as a function of the BST parameter ω, on the static (a) and dynamic (b) lattices, at $c = 0.9$.

Table 4. BST extrapolation of y_h/d, with the BST parameter $\omega = 1$, for the BEG model with $b = 9c/4(1+c^2)$ and $\tilde{x} = b\sqrt{3(1-c^4)}$ close to the edge $u_E = \mathrm{i}$ at different temperatures.

c	$y_h(\infty)$ (static)	$y_h(\infty)/d$ (dynamic)
0.1	2.000 000 0000(2)	2.000 000 0001(8)
0.65	2.00(1)	2.00(2)
$\sqrt{2}/2$	2.000 000 00(1)	1.999 999 999 9999(4)
0.75	3.0000(1)	3.0000(4)
0.9	3.000 0000(3)	3.000 0000(6)

4. Conclusion

First of all, we have verified numerically in a $\mathbb{Z}_2$ symmetric 1D spin model that even when the magnetic field is not pure imaginary (no circle theorem) we still have the Yang–Lee edge critical exponent $\sigma \approx -1/2$ in most of the cases. This is in agreement with a recent proof presented in [8], see also [9], based on the transfer matrix approach. In the dynamic case, including non-connected rings, although we have an expression for the partition function based on the transfer matrix eigenvalues of the static case, see (20), such expression is apparently too complicated to allow us a direct generalization of [8] to non-connected rings. So we have to stick to numerical results which still lead, usually, to $\sigma \approx -1/2$. Thus, the universality of the Yang–Lee edge singularity seems to go beyond static lattices for one-dimensional spin models. We must mention at this point that the situation is different in the $d = 2$ case, see [24], where the dynamics of the lattice (non-connected Feynman diagrams) leads apparently to the mean field result $\sigma = +1/2$ instead of $\sigma = -1/6$ which is the result predicted in [25] via conformal field theory and confirmed numerically, see e.g. [26, 27], for the $s = 1/2$ Ising model on static lattices.

Second, by fine tuning the couplings b and x of the BEG model to achieve triple degeneracy of the transfer matrix eigenvalues $\lambda_1 = \lambda_2 = \lambda_3$, we have found once again, see [9], a new

critical behavior with $\sigma = -2/3$ for both the static and the dynamic lattices. This is an indication that the new critical behavior, whenever available, is as much universal as the usual result $\sigma = -1/2$ and holds also for dynamic lattices.

As in [9], we have found that whenever the new critical behavior ($\sigma = -2/3$) is present at some edge singularity, we have another edge singularity with the usual exponent $\sigma = -1/2$. However, differently from [9], in the second example analyzed here (case II), above some temperature ($c > \sqrt{2}/2$), the new critical behavior appears at the closest edge to the positive real axis. Those facts may be relevant in the development of a possible tricritical version of the $\imath\varphi^3$ field theory which describes the usual critical behavior of the Yang–Lee edge singularity.

Last, at $c = \sqrt{2}/2$ and $b, \tilde{x}$ given in (30) and (31), we have shown exactly that, although we have triple degeneracy of the transfer matrix eigenvalues we still have the usual critical behavior with $y_h = 2(\sigma = -1/2)$. Therefore, the triple degeneracy condition $\lambda_1 = \lambda_2 = \lambda_3$, though necessary for a new critical behavior, is not a sufficient condition in general.

Acknowledgments

DD is partially supported by CNPq and FLS is supported by CAPES. A discussion with N A Alves on the BST extrapolation method is gratefully acknowledged.

References

[1] Yang C N and Lee T D 1952 *Phys. Rev.* **87** 404
Lee T D and Yang C N 1952 *Phys. Rev.* **87** 410
[2] Fisher M 1978 *Phys. Rev. Lett.* **40** 1610
[3] De Alcantara Bonfim O F, Kirkham J E and McKane A J 1980 *J. Phys. A: Math. Gen.* **13** L247
[4] Glumac Z and Uzelac K 1994 *J. Phys. A: Math. Gen.* **27** 7709
[5] Kurze D A 1983 *J. Stat. Phys.* **30** 15
[6] Fisher M 1980 *Suppl. the Progr. Theor. Phys.* **69** 14
[7] Wang X-Z and Kim J S 1998 *Phys. Rev.* E **58** 4174
[8] Ghulghazaryan R G, Sargsyan K G and Ananikian N S 2007 *Phys. Rev.* E **76** 021104
[9] Dalmazi D and Sá F L 2008 New critical behavior at edge singularities in one dimensional spin models *Phys. Rev.* E **78** 031138
[10] Almeida L A F and Dalmazi D 2005 *J. Phys. A: Math. Gen.* **38** 6863
[11] Bachas C, de Calan C and Petropoulos P 1994 *J. Phys. A: Math. Gen.* **27** 6121
Dolan B P, Janke W, Johnston D A and Stathakopoulos M 2001 *J. Phys. A: Math. Gen.* **34** 6211
[12] de Albuquerque L C and Dalmazi D 2003 *Phys. Rev.* E **67** 66108
de Albuquerque L C, Alves N A and Dalmazi D 2000 *Nucl. Phys.* B **580** 739
[13] Blume M, Emery V J and Griffiths R B 1971 *Phys. Rev.* A **4** 1071
[14] Blume M 1966 *Phys. Rev.* **141** c17
Capel H W 1966 *Physica* **32** 966
[15] Wu F Y 1992 *Chinese J. Phys.* **30** 157
[16] Ryder L H 1996 *Quantum Field Theory* (Cambridge: Cambridge University Press)
[17] Itzykson C, Pearson R B and Zuber J B 1983 *Nucl. Phys.* B **220** 415
[18] Creswick R J and Kim S-Y 1997 *Phys. Rev.* E **56** 2418
[19] Lassettre E N and Howe J P 1941 *J. Chem. Phys.* **9** 747
[20] Ashkin J and Lamb W E 1943 *Phys. Rev.* **64** 159
[21] Bulirsch R and Stoer J 1964 *Numer. Math.* **6** 413
[22] Henkel M and Schutz G 1988 *J. Phys. A: Math. Gen.* **21** 2617
[23] Kim S-Y 2005 *Nucl. Phys.* B **705** 504
[24] Johnston D A 1998 *J. Phys. A: Math. Gen.* **31** 5641–50
[25] Cardy J L 1985 *Phys. Rev. Lett.* **54** 1354
[26] Matveev V and Schrock R 1996 *Phys. Rev.* E **53** 254
[27] Kim S-Y 2006 *Phys. Rev.* E **74** 011119